

Proc. of the International Conference on Mechanochemistry and Mechanical Alloying, Kraków, Poland, June 22–26, 2014

# Mechanosynthesis of Nanocomposites Based on Fe–TiC and Fe–TiN in Hydrocarbon Medium

K. YAZOVSKIKH\*, S.F. LOMAYEVA AND A.V. SYUGAEV

Physical-Technical Institute, Ural Branch of Russian Academy of Sciences, Izhevsk, Russia

In this paper the nanocomposites based on Fe–TiC and Fe–TiN which were produced by mechanochemistry of the mixture of Fe or Fe–N (82 at.%) and Ti (18 at.%) in toluene for 16 h and subsequent compaction have been studied. The structural-phase composition and morphology of the mechanochemically synthesized powders were studied by X-ray diffraction analysis, the Mössbauer spectroscopy and electron microscopy. It has been shown that powders of the following composition: a solid solution based on Fe, TiC or TiN, a phase on the basis of  $\text{Fe}_3\text{C}$  — are formed by mechanochemistry. The measurements of microhardness and corrosion resistance of the produced compacts were carried out as well.

DOI: [10.12693/APhysPolA.126.1053](https://doi.org/10.12693/APhysPolA.126.1053)

PACS: 81.05.Mh, 81.20.Ev, 82.45.Bb, 61.05.Qr

## 1. Introduction

At present the development of alloys characterized by high hardness, wear and corrosion resistance for manufacturing various structural parts or coatings that operate under high mechanical loads and aggressive environments is of great interest. Perspective materials are metal alloys toughened by ceramic particles — carbides, nitrides, oxides of refractory metals, which possess unique physical properties including high hardness, thermal and chemical stability [1–3].

Mechanochemically synthesized composites based on metal–ceramics have unique properties and cannot be produced by conventional metallurgical techniques. A nanocrystalline structure, through which more opportunities to improve useful properties of such composites can be implemented, is of considerable importance.

The structural-phase composition of the mechanochemically synthesized samples and the influence of the type of reinforcing ferrite matrix particles on the physical and chemical properties of compacts have been studied in this paper.

## 2. Experimental procedure

### 2.1. Preparation of Fe–TiC and Fe–TiN composites

The samples were produced by mechanochemistry (MS) of the powder mixtures:

1) 82 at.% Fe (99.95% purity, an average particle size was about  $10\mu\text{m}$ ) and 18 at.% Ti in toluene for 16 h (Fe–TiC composite);

2) 82 at.% Fe–N (Fig. 1) and 18 at.% Ti in toluene for 16 h (Fe–TiN composite).

MS was carried out using Fritsch “Pulverisette 7” planetary ball mill. The mill vials and grinding balls were

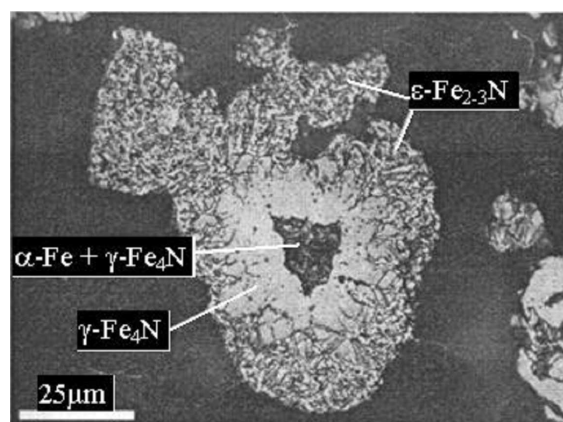


Fig. 1. The metallographic examination of nitrided iron (Fe–31 at.% N).

made of hardened steel, which has a minimum content of alloying elements. The weight of the initial downloaded powder was 10 g. The volume of the mill vial left was filled with toluene taken as a carbon source. The samples were milled for 20 h.

The mechanochemically synthesized powders were compacted by the method of magnetic pulse compaction [4, 5] in vacuum at the temperature of  $500^\circ\text{C}$ . The compacts produced were of a disk form, their diameter being of 15 mm and thickness being equal to 2 mm.

### 2.2. Characterization of Fe–TiC and Fe–TiN composites

The X-ray diffraction (XRD) measurements were carried out using a DRON-3M diffractometer ( $\text{Cu } K_\alpha$  radiation). The software packages [6] were used to perform qualitative and quantitative XRD analyses as well as to determine the lattice parameters. The Mössbauer spectra were obtained in the constant acceleration mode using a NGRS-4M spectrometer with a  $^{57}\text{Co}(\text{Cr})$  source.

\*corresponding author; e-mail: [pti@mail.ru](mailto:pti@mail.ru), [uds@ftiudm.ru](mailto:uds@ftiudm.ru)

The  $P(H)$  distribution functions of the magnetic hyperfine fields were found by the generalized regular algorithm [7]. The metallographic examination was carried out using a LEO 982 scanning electron microscope. The polished samples were etched by a 3% nitric acid solution in alcohol. The microhardness of the compacts was measured by the method of Vickers diamond pyramid indentation using a mechanical properties measuring device, Nanotest 600. The corrosion resistance of the compacts was studied by potentiodynamic method using an IPC-Pro potentiostat at room temperature. The measurements were carried out in a borate solution with  $\text{pH} = 7.4$ .

### 3. Results and discussion

In the X-ray pattern of the Fe–TiC powder after MS  $\alpha$ -Fe and TiC reflections strongly broadened are presented (Fig. 2a). The formed TiC is characterized by the low value of the lattice parameter due to the low concentration of carbon in the monocarbide (Table I). The lattice parameter of  $\alpha$ -Fe increases up to 0.2877 nm comparing to the original iron lattice parameter (0.2866 nm). The most likely reason for the increase of the lattice parameter is the partial dissolution of Ti ( $\approx 3$  at.%) in  $\alpha$ -Fe [8]. The data of the XRD analysis are well agreed with the data obtained by the method of the Mössbauer spectroscopy. In the functions  $P(H)$ , recovered from the Mössbauer spectra, the peaks related to  $\alpha$ -Fe and alloying  $\alpha$ -Fe by Ti atoms (300  $\div$  320 kOe) are revealed (Fig. 3a).

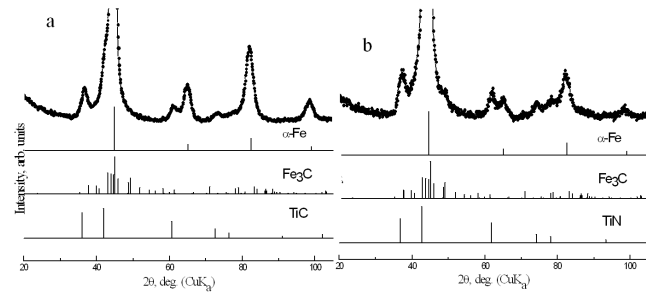


Fig. 2. X-ray pattern of the powders after MS: (a) Fe–TiC, (b) Fe–TiN.

The sequence of structural and phase transformations during MS of the Fe and Ti powders in toluene can be presented as the formation of the nanocrystalline structure in the particles of  $\alpha$ -Fe and Ti, the dissolution of Ti in  $\alpha$ -Fe, the thermocatalytic destruction of toluene at newly formed metal surface, the formation of mostly TiC for which the enthalpy of formation,  $\Delta H(\text{TiC}) = -209$  kJ/mol, is much smaller than that for cementite,  $\Delta H(\text{Fe}_3\text{C}) = 25$  kJ/mol. Once the total amount of the free Ti forms carbide, the carbon which is being released due to toluene destruction is related to Fe with  $\text{Fe}_3\text{C}$  formation.

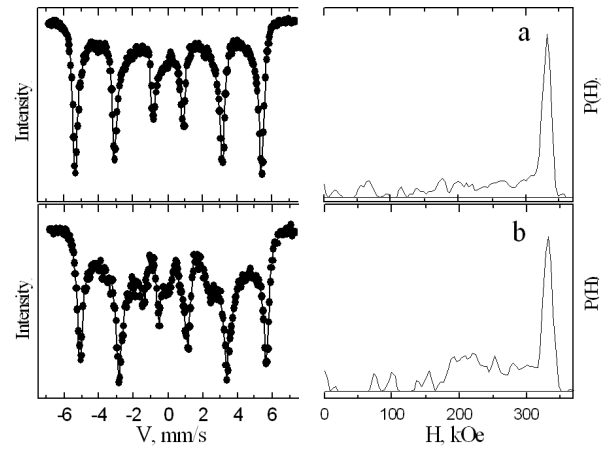


Fig. 3. Mössbauer spectra and  $P(H)$  functions: (a) Fe–TiC, (b) Fe–TiN.

TABLE I

XRD analysis results: the powders after MS.

Sample	Phase composition	wt% ( $\pm 5\%$ )	Lattice parameters [nm] $\pm 0.5$ pm	Grain size $\langle L \rangle$ [nm] $\pm 1$
Fe–TiC	$\alpha$ -Fe	68	0.2877	8
	TiC	23	0.4288	6
	$\text{Fe}_3\text{C}$	9	*	*
Fe–TiN	$\alpha$ -Fe	38	0.2874	6
	TiN	27	0.4222	5
	$\text{Fe}_3\text{C}$	35	*	*

\*The lattice parameters and grain size could not be determined because of the strong broadening of the lines

MS of the mixture of Fe–N and Ti in toluene results in the formation of complicated phase composition powders (Fig. 2b, 3b; Table I), i. e. a solid solution based on  $\alpha$ -Fe, non-stoichiometric TiN and  $\text{Fe}_3\text{C}$ . Under conditions of severe plastic deformation at MS primary nitrated iron disorders and loses nitrogen. Next step is the TiN phase formation ( $\Delta H(\text{TiN}) = -323$  kJ/mol) as long as the system has free titanium. The carbon which is released due to toluene destruction, bonds to Fe, forming  $\text{Fe}_3\text{C}$ .

Images of the surface of the Fe–TiC and Fe–TiN compacts after chemical etching (Fig. 4) do not differ qualitatively. Compacts consist of fragments with an average size,  $\approx 40\mu\text{m}$ , which corresponds to the size of the powder particles after MS. Small globular and large inclusions of a faceted shape characteristic for TiC and TiN are seen at higher magnification.

Figure 5 and Table II show the results of XRD analysis. The X-ray patterns of the Fe–TiC and Fe–TiN compacts show broadened  $\alpha$ -Fe and  $\text{Fe}_3\text{C}$  reflexions along with TiC and TiN reflexions, respectively.

Microhardness of the Fe–TiC compact is 13.5 GPa at a density of 96% of the theoretical one (Table III). The highest microhardness was obtained using the Fe–TiC compact.

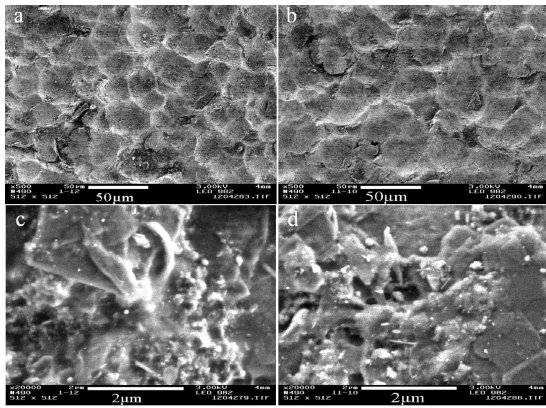


Fig. 4. Electron microscopy images of the compacts: (a) Fe-TiC, (b) Fe-TiN.

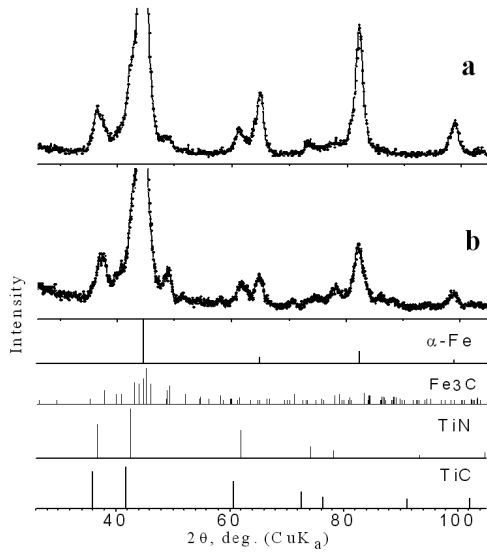


Fig. 5. X-ray pattern of the compacts: (a) Fe-TiC, (b) Fe-TiN.

One of the most important factors determining the corrosion resistance in neutral media is the resistance of the formed passive films to the action of ions provoking pitting corrosion and, above all, to the action of chloride ions. Figure 6 shows the corrosion resistance test results of Fe and compacts in borate solution ( $\text{pH} = 7.4$ ) with 0.01 M NaCl. Passive film breakdown potential of the Fe-TiC compact is 200 mV higher than that of Fe. This indicates a higher stability of the passive film on the Fe-TiC compact (consist mainly of FeO-TiO<sub>2</sub> mixed oxides [9]) to the destructive action of chloride ions compared to the passive film on Fe. Passive film on Fe-TiN compact has even higher corrosion resistance. This can be explained by the additional inclusion of nitrogen particles in its composition and the formation of the Fe-O-NO<sub>x</sub> structures [10-13].

Similar results were obtained in studies of corrosion resistance of Fe and compacts in borate solution,  $\text{pH} = 7.4$  without adding 0.01 M NaCl (Fig. 7). Passive film on Fe-TiN compact has the highest corrosion resistance.

TABLE II

XRD analysis results: the compacts.

Sample	Phase composition	wt% ( $\pm 5\%$ )	Lattice parameters [nm] $\pm 0.5$ pm	Grain size $\langle L \rangle$ [nm] $\pm 1$
Fe-TiC	$\alpha$ -Fe	64	0.2877	11
	TiC	24	0.4259	6
	Fe <sub>3</sub> C	12	*	*
Fe-TiN	$\alpha$ -Fe	35	0.2877	9
	TiN	27	0.4222	6
	Fe <sub>3</sub> C	38	*	*

\*The lattice parameters and grain size could not be determined because of the strong broadening of the lines

TABLE III

Microhardness  $H_v$  and density  $\rho$  of the compacts.

Sample	$\rho$ [g/m <sup>3</sup> ] $\pm 0.1$		$H_v^{200}$ GPa
	Exp.	Theor.*	
Fe-TiC	6.8	7.1	13.5 $\pm$ 0.7
Fe-TiN	6.8	7.2	12.1 $\pm$ 0.7

\*Theoretical density from X-ray data

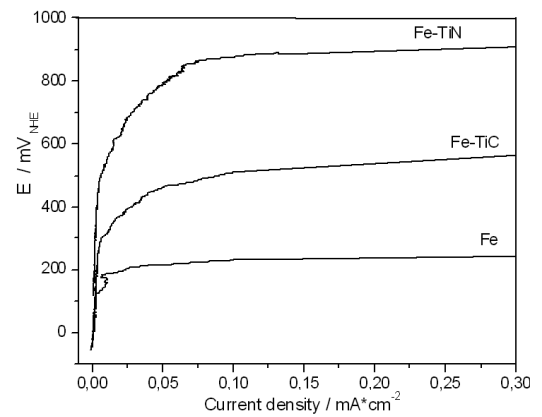


Fig. 6. Anodic curves of Fe and compacts in borate solution,  $\text{pH} = 7.4$ , with 0.01 M NaCl.

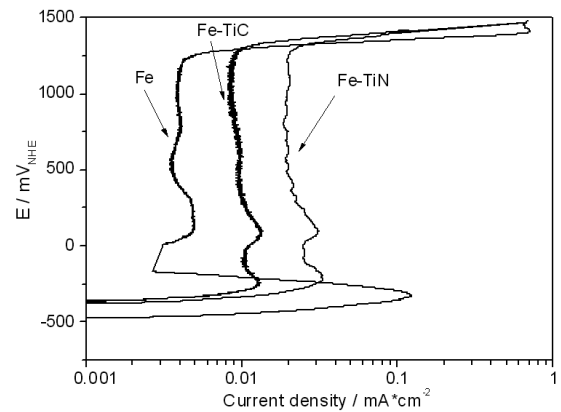


Fig. 7. Anodic curves of Fe and compacts in borate solution,  $\text{pH} = 7.4$ , without adding 0.01 M NaCl.

#### 4. Conclusions

Mechanosynthesis of the mixture of Fe (or Fe–N) and Ti in toluene for 16 h has been shown to result in the formation of the complicated phases composition nanocomposites. The phases are presented as a solid solution based on  $\alpha$ -Fe, non-stoichiometric TiC or TiN and a phase on the basis of Fe<sub>3</sub>C.

The produced compacts have a number of important practical physical and chemical properties. On reinforcing the ferrite matrix by the TiC particles predominantly the produced nanocomposite shows the highest microhardness, 13.5 GPa at a density of 96% of the theoretical one.

The reinforcing of the ferrite matrix by the TiN particles leads to high corrosion resistance in neutral media, which are the most important for practical applications of produced nanocomposites.

#### Acknowledgments

The authors would like to thank A.S. Yurovskikh (Ural Federal University, Yekaterinburg, Russia) for produced powders of nitrided iron.

#### References

- [1] A. Nilsson, L. Kirkhorn, M. Andersson, J.-E. Stahl, *Wear* **271**, 1280 (2011).
- [2] M. Sheikhzadeh, S. Sanjabi, *Mater. Des.* **39**, 366 (2012).
- [3] H.-J. Cho, S.-Y. Bae, I.-S. Ahn, D.-K. Park, *Mater. Sci. Forum* **544-545**, 825 (2007).
- [4] V.V. Ivanov, S.N. Paragin, A.N. Vikhrev, *Russian Patent No. 2083328*, 1996.
- [5] V.V. Ivanov, A.S. Kaygorodov, V.R. Khrustov, S.N. Paragin, in: *Ceramic Materials — Progress in Modern Ceramics*, Ed. Feng Shi, InTech, Rijeka 2012, p. 43.
- [6] Powder Diffraction File, Alphabetical Index, Inorganic Phases (International Center for Diffraction Data, 1601 Park Lane, Swarthmore, Pennsylvania 19081, USA), 1985.
- [7] E.V. Voronina, N.V. Ershov, A.L. Ageev, Yu.A. Babanov, *Phys. Status Solidi B* **160**, 625 (1990).
- [8] A.E. Vol, *Structure and Properties of Binary Metallic Systems*, FIZMATLIT, Moscow 1962.
- [9] A.V. Syugaev, S.F. Lomaeva, N.V. Lyalina, S.M. Reshetnikov, *Protect. Met. Phys. Chem. Surf.* **47**, 590 (2011).
- [10] F.Z. Bouanis, C. Jama, M. Traisnel, F. Bentiss, *Corros. Sci.* **52**, 3180 (2010).
- [11] A. Basu, J. Dutta Majumdar, J. Alphonsa, S. Mukherjee, I. Manna, *Mater. Lett.* **62**, 3117 (2008).
- [12] J. Flis, I. Flis-Kabulska, T. Zakroczymski, *Electrochim. Acta* **54**, 1810 (2009).
- [13] L. Wang, Y. Li, X. Wu, *Appl. Surf. Sci.* **254**, 6595 (2008).